Acta Crystallographica Section D
Biological Crystallography
ISSN 0907-4449

Purification, crystallization and X-ray diffraction analysis of the extracellular part of the human Fc receptor for IgA, FcαRI (CD89)

Katja Wenig and Peter Sondermann*

Max-Planck-Institut für Biochemie, Abteilung Strukturforschung, Am Klopferspitz 18a, 82152 Martinsried, Germany

Correspondence e-mail: sonderma@biochem.mpg.de

Received 30 April 2003
Accepted 24 July 2003

FcαRI is the predominant receptor for IgA in the serum. Nevertheless, the interaction between the molecules that finally leads to an immune response is poorly understood. To investigate the structural requirements for IgA binding, the extracellular region of FcαRI was cloned and overexpressed in *Escherichia coli*. The resulting inclusion-body protein was refolded and purified. Despite its deglycosylated state, this recombinant FcαRI retained its ability to bind human IgA. The protein crystallized spontaneously as microcrystalline needles. Recrystallization yielded crystals belonging to a primitive monoclinic space group. A complete 2.8 Å resolution X-ray diffraction data set was collected using synchrotron radiation.

1. Introduction

Antibodies are important mediators of the humoral immune response. These highly specific Y-shaped proteins recognize antigenic structures present in pathogens with their variable domains, which are located at the tip of the Fab fragments. The Fc region linked to these Fab fragments *via* the flexible hinge peptides is responsible for eliciting various effector functions. Interaction of the Fc portion with complement proteins mediates the humoral immune response, whereas a wide range of cellular effector functions is triggered *via* the binding to Fc receptors present on all immunologically active cells. Important cellular effects include the activation of B cells, endocytosis and phagocytosis of immune complexes and antibody-dependent cellular cytotoxicity (ADCC).

Of the five different immunoglobulin classes in man, IgA represents the main antibody in mucosal tissues. In fact, more IgA is produced per day than all other immunoglobulin isotypes combined (>60 mg kg^{-1} per day; Mestecky & McGhee, 1987). Nevertheless, relatively little is known about the nature and function of IgA, while the roles of IgG and IgE including their receptors are well characterized and are also understood from structural studies (Sondermann *et al.*, 2000; Garman *et al.*, 2000)

In human serum, IgA circulates predominantly in the monomeric form, whereas in mucosal sites it occurs almost exclusively as a dimer (sIgA) in complex with two additional peptides, termed J-chain and secretory component, the latter being the extracellular ligand-binding fragment of the poly-immunoglobulin receptor (pIgR; Mostov, 1994). Interestingly, three structurally unrelated IgA-binding Fc receptors exist in humans, the aforementioned pIgR (Eiffert *et al.*, 1991), the recently identified Fcα/μR (Shibuya *et al.*, 2000) and the myeloid-specific FcαRI (CD89) (Maliszewski *et al.*, 1990).

Many different human cell types express FcαRI, especially macrophages and myeloid cells, *e.g.* neutrophils, eosinophils and monocytes (Fanger *et al.*, 1980). The aggregation of FcαRI by serum IgA containing immune complexes results in phagocytosis and the release of inflammatory mediators and cytokines. FcαRI is a type I transmembrane protein, which comprises two extracellular Ig-like domains responsible for ligand binding, a transmembrane region and a short cytoplasmic tail (van Egmond *et al.*, 2001).

While pIgR mediates the transcytosis of IgA into mucosal secretions and the function of Fcα/μR is not yet clearly understood, FcαRI seems to be mainly responsible for the IgA-mediated immune response in the serum.

FcαRI has a low affinity towards its ligands IgA1 and IgA2 ($K_a \simeq 10^6\ M^{-1}$) and towards both monomeric and polymeric IgA. With regard to its function FcαRI can be described as a classical Fc receptor, but its sequence similarity to killer-cell inhibitory receptors (KIR; ~32% identity) and leukocyte-inhibitory receptors (LIR; ~35% identity) and the location of the FcαRI gene at chromosome 19q13.4 in humans points to a more KIR/LIR-related immune receptor. Another difference is that the ligand-binding site of FcαRI has been mapped to the N-terminal Ig domain by mutagenesis studies (Wines *et al.*, 1999), while the FcγRs mainly use the second Ig domain for ligand binding (Sondermann *et al.*, 2000). The binding site for FcαRI on IgA seems to overlap with that of bacterial IgA-binding proteins, pointing to the Cα2/Cα3 interdomain region (Pleass *et al.*, 2001). Such a model is consistent

with a study that revealed a 2:1 stoichiometry for the FcαRI–IgA-Fc interaction (Herr, White *et al.*, 2003).

The scientific interest in IgA and its receptors has increased recently owing to the fact that human cancers can be very effectively treated with therapeutic IgA antibodies (Dechant & Valerius, 2001), which mediate the lysis of tumour cells by binding to FcαRI present on polymorphonuclear neutrophils.

Because of these findings, the three-dimensional structure of this protein is of great interest and awaits solution. Here, we report the refolding, purification, crystallization and preliminary X-ray data collection of the extracellular IgA-binding region of human FcαRI.

2. Protein expression and purification

The DNA fragment coding for the extracellular domain of FcαRI was cloned by polymerase chain reaction (PCR) using the 5′-primer 5′-AAAAAAA**CATATG**CAGGCACAGGAAGG-3′ and the 3′-primer 5′-AAAA**GGATCC**TAGTTCTGCGTCGTGTAATC-3′ (restriction sites are in bold) from a λ-phage cDNA bank prepared from buffy coat (kindly provided by T. Matthias). The derived gene was cloned as an *Nde*I–*Bam*HI fragment into the pET22b+ vector (Novagen, Darmstadt, Germany) and sequenced for verification. For overexpression in *Escherichia coli*, the recombinant plasmid was transformed into the bacterial strain Rosetta (DE3) (Novagen, Darmstadt, Germany).

Expression, inclusion-body preparation and refolding were performed as described previously (Sondermann & Jacob, 1999). Briefly, *E. coli* cells harbouring the plasmid were grown in Luria–Bertani medium containing the respective antibiotics at 310 K and were induced with 1 m*M* isopropyl-β-D-thiogalactopyranoside at an OD_{600nm} of 0.8. After further growth for 4 h, the bacteria were pelleted, resuspended in 100 m*M* Tris–HCl pH 7.5, 150 m*M* sodium chloride and 0.02% sodium azide and treated with lysozyme for 30 min at room temperature. Subsequently, 0.5 volumes of the wash buffer containing 0.5% *N*,*N*-dimethyldodecylamine *N*-oxide (LDAO), 100 m*M* Tris–HCl pH 7.5 were added and the cells were sonicated intensely.

Under these conditions, the expressed receptor fragment was deposited in inclusion bodies, which were isolated by centrifugation at 32 000*g* and 277 K for 20 min. Subsequently, inclusion bodies were resuspended repeatedly in wash buffer (see above) with an Ultra-Turrax-T25 Basic (IKA, Staufen, Germany) and centrifuged. Finally, the LDAO was removed completely by a further wash with a buffer containing 100 m*M* Tris–HCl, 1 m*M* EDTA pH 7.5 and the inclusion bodies (Fig. 1*a*) were solubilized in 6 *M* guanidinium hydrochloride, 100 m*M* DTT, 100 m*M* Tris–HCl pH 8.0 to a protein concentration of 35 mg ml^{-1} and separated from the insoluble matter by centrifugation. Refolding was achieved by the rapid dilution method. 10 ml of protein solution was added dropwise in five pulses (2 ml each) to 1 l of refolding buffer (1.0 *M* arginine, 100 m*M* Tris–HCl, 5 m*M* reduced glutathione, 0.02% sodium azide pH 8.5 at 283 K), which was stirred continuously. The mixture was then stirred for 4–5 d until the concentration of free thiol groups was reduced to 1 m*M* by air oxidation, which was measured by Ellman's method (Ellman, 1959).

Precipitate formed during the refolding procedure was removed by centrifugation for 20 min at 277 K and 32 000*g*. The protein solution was concentrated 20-fold in a stirred-cell concentrator (Millipore, Schwalbach, Germany) using a 5 kDa molecular-weight cutoff (MWCO) membrane and rebuffered to 2 m*M* Tris–HCl pH 8.0. In the final purification step, the sample was loaded onto a Superdex-75 gel-filtration column (Amersham Biosciences, Uppsala, Sweden) equilibrated with 2 m*M* Tris–HCl, 20 m*M* NaCl pH 8.0. Fractions containing FcαRI were pooled, rebuffered to 2 m*M* Tris–HCl pH 8.0, concentrated to 5 mg ml^{-1} by ultrafiltration (MWCO 5 kDa, Millipore, Schwalbach, Germany) and stored at 277 K for crystallization trials. The homogeneity of the protein was assessed by SDS–PAGE and Coomassie Blue staining (Fig. 1*a*).

The activity of the refolded material was tested by affinity chromatography with IgA Sepharose, while IgG Sepharose served as a negative control. After binding in phosphate-buffered saline (PBS) and two washing steps under the same conditions, the bound material was eluted with 100 m*M* glycine at pH 3.0 (Fig. 1*b*). Interestingly, under these conditions the unglycosylated FcαRI shows specific and quantitative binding to IgA, indicating a homogeneous and active material.

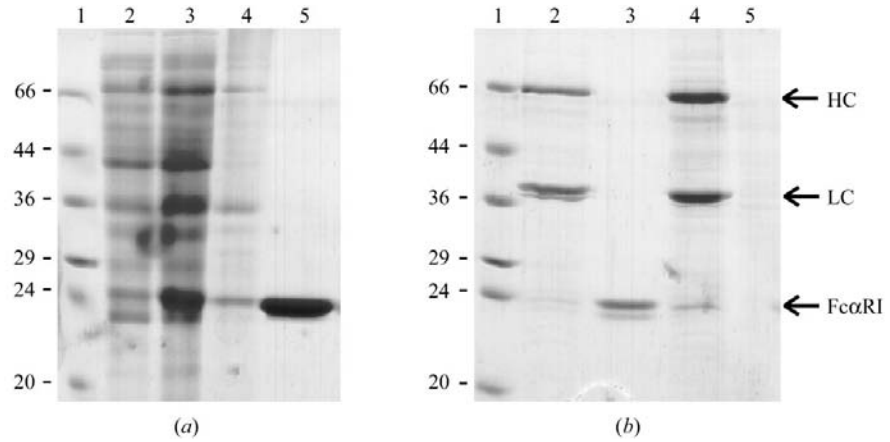

Figure 1
(*a*) Expression and purification of FcαRI: molecular-weight markers (lane 1), uninduced (lane 2) and induced (lane 3) cell lysate, purified inclusion bodies (lane 4), purified refolded FcαRI (lane 5). (*b*) A solution of FcαRI was incubated with either IgA or IgG Sepharose: molecular-weight markers (lane 1), IgA Sepharose flowthrough (lane 2), IgA Sepharose elution (lane 3), IgG Sepharose flowthrough (lane 4), IgG Sepharose elution (lane 5). LC, light chain; HC, heavy chain.

3. Crystallization

The storage of the protein solution at 277 K for 2 d resulted in the formation of crystalline needles (Fig. 2*a*). Unfortunately, these crystals were too small for X-ray diffraction studies (maximum dimension of 10 µm). However, we used this crystallization as a further purification procedure, which included several washing steps of these needles with water.

The protein crystals could be dissolved up to a protein concentration of 5 mg ml^{-1} in 100 m*M* citrate pH 6.0 but not in other buffers. For recrystallization, various precipitants were tested, keeping citrate as the buffer system. This was performed by mixing 1.5 µl of protein solution in Cryschem trays (Charles Supper Co., Natick, MA, USA) with an equal volume of the reservoir solution using the sitting-drop vapour-diffusion technique. Optimization of the crystallization condition yielded the best crystals in 100 m*M* citrate pH 6.0, 4%(*v*/*v*) ethylene glycol at a temperature of 293 K with a

protein concentration of 5 mg ml^{-1}. The rhomboid-shaped crystals (Fig. 2*b*) were visible after 1–2 d and reached maximum dimensions of approximately 0.2 × 0.1 × 0.04 mm after 1–2 weeks.

4. Data collection

Prior to cryocooling, the crystals were carefully transferred into 2 µl cryoprotectant [reservoir solution containing 12% D(−)-2,3-butanediol] for 5–10 s.

All data sets were collected at a temperature of 100 K on the wiggler beamline BW6 at the Deutsches Elektronen Synchrotron (DESY Hamburg, Germany) using a MAR 165 mm CCD detector (MAR Norderstedt, Germany). FcαRI crystals diffracted to a limiting resolution of about 2.5 Å. Some of the measured crystals were indexed with *DENZO* (Otwinowski & Minor, 1997) in a *C*-centred orthorhombic lattice, with unit-cell parameters a = 53.1, b = 144.9, c = 140.7 Å (Table 1). The merging of the data with *SCALEPACK* led to a reasonable R_{sym} of 6.1%. However, a plot of the cumulative intensity distribution of the acentric data (Fig. 3*a*) showed a sigmoid progression, which is characteristic of twinned crystals. The presence of twinning can also be detected by analysis of the second moment of intensities, where values of 2.0 and 1.5 are expected for untwinned data and perfectly twinned crystals, respectively (Declercq & Evrard, 2001). Fig. 3(*b*) shows the second moment of intensities as a function of resolution. Its average value of 1.67 suggests partial twinning.

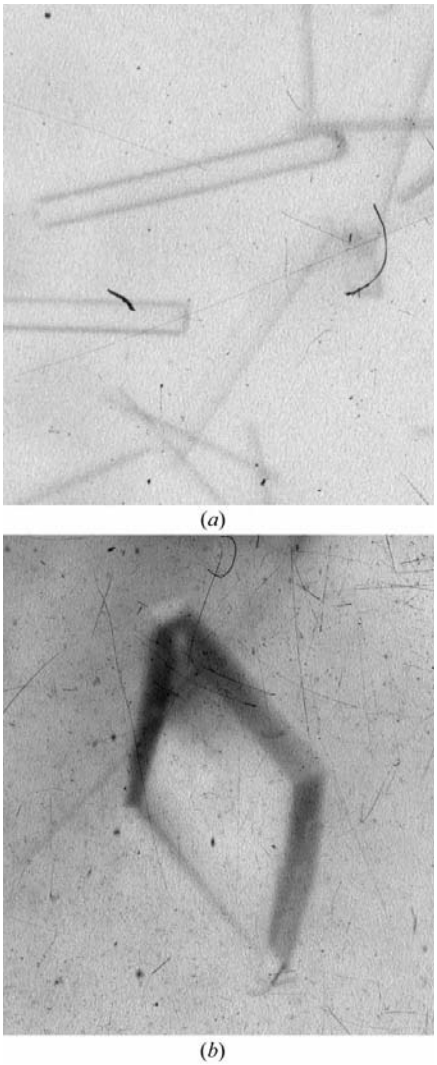

Figure 2
Crystals of FcαRI. (*a*) Needles obtained after 2 d storage in 2 m*M* Tris–HCl pH 8.0. (*b*) Rhomboid-shaped crystals recrystallized in 100 m*M* citrate pH 6.0, 4% ethylene glycol.

The X-ray data collected from the second set of crystals (obtained from identical crystallization conditions) could not be processed in a *C*-centred orthorhombic lattice. Instead, the pattern indicated a primitive monoclinic crystal system, with unit-cell parameters a = 53.1, b = 140.6, c = 77.2 Å, β = 110°. Assuming four molecules of FcαRI (22.8 kDa) per asymmetric unit, the Matthews coefficient (V_M) was calculated to be 2.96 Å^3 Da^{-1}, corresponding to a solvent content of 58% (Matthews, 1968). The second moment of intensities (1.99; Fig. 3*b*) and the cumulative intensity distribution plot (Fig. 3*a*) of this data set indicated untwinned data. Interestingly, the unit-cell parameters of this crystal fulfil the geometrical relationship ($c\cos\beta = -a/2$) required for simulating the orthorhombic Laue group *mmm* in the case of perfect twinning (see, for example, Fig. 1*a* in Declercq & Evrard, 2001). Additionally, it has been pointed out that non-crystallographic symmetry (NCS) may promote twinning (Larsen *et al.*, 2002; Royant *et al.*, 2002). Accordingly, self-rotation Patterson searches revealed two non-crystallographic twofold axes orthogonal to each other and to the crystallographic twofold axis of the monoclinic crystal using *POLARRFN* (Collaborative Computational Project, Number 4, 1994). Considering the transformation between the two apparent lattice types, these twofold NCS axes are parallel to the crystallographic axes observed in the *C*-centred orthorhombic lattice. With regard to these findings, we conclude that the

Table 1
Summary of crystallographic data collection and processing.

Values in parentheses refer to the highest resolution shell (2.96–2.8 Å for $P2_1$ and 2.59–2.5 Å for $C222_1$).

Crystal	Monoclinic, untwinned	Pseudo-orthorhombic, twinned
Space group	$P2_1$	$C222_1$ (for processing)
Unit-cell parameters (Å, °)	a = 53.1, b = 140.6, c = 77.2, $\alpha = \gamma = 90$, β = 110	a = 53.1, b = 144.9, c = 140.2, $\alpha = \gamma = \beta = 90$
Mosaicity (°)	2.1	1.1
Wavelength (Å)	1.05	1.05
Resolution range (Å)	20.0–2.8	20.0–2.5
Observations	41514	44080
Unique reflections	22945	17600
Completeness (%)	88.4 (83)	91.5 (76.3)
Average $I/\sigma(I)$	11.6 (5.01)	19.6 (5.6)
R_{sym} (%)	5.1 (11.0)	6.0 (19.8)
Second moment of intensities	1.99	1.67

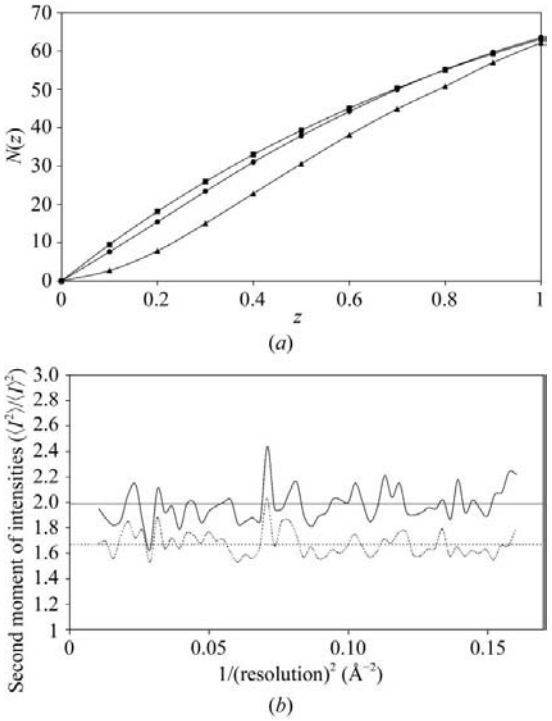

Figure 3
(*a*) Cumulative intensity distribution of acentric data: $N(z)$ is the percentage of reflections with $I/\langle I\rangle \leq z$. Theoretical values for untwinned data are depicted with squares and values for observed data with triangles for the twinned crystal and dots for the untwinned crystal. (*b*) Second moment of the intensities ($\langle I^2\rangle/\langle I\rangle^2$) as a function of resolution of the twinned data set (dashed line) and the untwinned data set (solid line).

initially assumed orthorhombic symmetry is only a pseudosymmetry caused by twinning and that the true space group is monoclinic. Detailed crystal parameters and data-collection statistics of both data sets are summarized in Table 1. Owing to the large mosaicity, the data were cut off at 2.8 Å resolution in the monoclinic and 2.5 Å resolution in the orthorhombic form to avoid spot overlap. The second untwinned $P2_1$ crystal form was used for further X-ray analysis. Despite the homology between FcαRI and KIR/LIR, the molecular-replacement approach with the use of several programs was unsuccessful.

Note added in proof: The structure of FcαRI has recently been described (Herr, Ballister *et al.*, 2003). Although a glycosylated form of the receptor has been used in this study, molecular replacement using these coordinates should facilitate the solution of our crystal structure.

The authors are indebted to Robert Huber for his generous support of this work and to Manuel Than for helpful discussion.

References

Collaborative Computational Project, Number 4 (1994). *Acta Cryst.* D**50**, 760–763.

Dechant, M. & Valerius, T. (2001). *Crit. Rev. Oncol. Hematol.* **39**, 69–77.

Declercq, J. P. & Evrard, C. (2001). *Acta Cryst.* D**57**, 1829–1835.

Egmond, M. van, Damen, C. A., van Spriel, A. B., Vidarsson, G., van Garderen, E. & van de Winkel, J. G. (2001). *Trends Immunol.* **22**, 205–211.

Eiffert, H., Quentin, E., Wiederhold, M., Hillemeir, S., Decker, J., Weber, M. & Hilschmann, N. (1991). *Biol. Chem. Hoppe-Seyler*, **372**, 119–128.

Ellman, G. L. (1959). *Arch. Biochem. Biophys.* **82**, 70–77.

Fanger, M. W., Shen, L., Pugh, J. & Bernier, G. M. (1980). *Proc. Natl Acad. Sci. USA*, **77**, 3640–3644.

Garman, S. C., Wurzburg, B. A., Tarchevskaya, S. S., Kinet, J. P. & Jardetzky, T. S. (2000). *Nature (London)*, **406**, 259–266.

Herr, A. B., Ballister, E. R. & Bjorkman, P. J. (2003). *Nature (London)*, **423**, 614–620.

Herr, A. B., White, C. L., Milburn, C., Wu, C. & Bjorkman, P. J. (2003). *J. Mol. Biol.* **327**, 645–657.

Larsen, N. A., Heine, A., de Prada, P., Redwan, E., Yeates, T. O., Landry, D. W. & Wilson, I. A. (2002). *Acta Cryst.* D**58**, 2055–2059.

Maliszewski, C. R., March, C. J., Schoenborn, M. A., Gimpel, S. & Shen, L. (1990). *J. Exp. Med.* **172**, 1665–1672.

Matthews, B. W. (1968). *J. Mol. Biol.* **33**, 491–497.

Mestecky, J. & McGhee, J. R. (1987). *Adv. Immunol.* **40**, 153–245.

Mostov, K. E. (1994). *Annu. Rev. Immunol.* **12**, 63–84.

Otwinowski, Z. & Minor, W. (1997). *Methods Enzymol.* **276**, 307–326.

Pleass, R. J., Areschoug, T., Lindahl, G. & Woof, J. M. (2001). *J. Biol. Chem.* **276**, 8197–8204.

Royant, A., Crizot, S., Kahn, R., Belrhali, H., Fieschi, F., Landau, E. M. & Pebay-Peyroula, E. (2002). *Acta Cryst.* D**58**, 784–791.

Shibuya, A., Sakamoto, N., Shimizu, Y., Shibuya, K., Osawa, M., Hiroyama, T., Eyre, H. J., Sutherland, G. R., Endo, Y., Fujita, T., Miyabayashi, T., Sakano, S., Tsuji, T., Nakayama, E., Phillips, J. H., Lanier, L. L. & Nakauchi, H. (2000). *Nature Immunol.* **1**, 441–446.

Sondermann, P., Huber, R., Oosthuizen, V. & Jacob, U. (2000). *Nature (London)*, **406**, 267–273.

Sondermann, P. & Jacob, U. (1999). *Biol. Chem.* **380**, 717–721.

Wines, B. D., Hulett, M. D., Jamieson, G. P., Trist, H. M., Spratt, J. M. & Hogarth, P. M. (1999). *J. Immunol.* **162**, 2146–2153.